STUDY OF THE TURBULENT MIXING ZONE INDUCED BY THE RICHTMYER-MESHKOV INSTABILITY USING LASER DOPPLER VELOCIMETRY AND SCHLIEREN VISUALIZATIONS

G. Bouzgarrou[1§], Y. Bury[1], S. Jamme[1], J.-F.Haas[2], L. Joly[1]
[1]Université de Toulouse, ISAE, 10 Avenue Edouard Belin, 31055 Toulouse, France
[2]CEA, DAM, DIF, F-91297 Arpajon, France
[§] ghazi.bouzgarrou@isae.fr

ABSTRACT An experimental study of the compressible mixing generated by the Richtmyer-Meshkov instability (RMI) is carried out in a vertical shock tube by means of two-components Laser Doppler Velocimetry (2C-LDV) measurements and Time-resolved Schlieren visualizations. An attempt is made to quantify the RMI-induced air/sulphurhexafluoride (SF6) mixing by measuring turbulence levels inside the mixing zone at a given stage of its development and by extracting the growth rate of the mixing zone from the Schlieren images.

Keywords **-** Richtmyer–Meshkov instability, turbulent mixing zone, shock tube, LDV, Schlieren visualizations

INTRODUCTION

The Richtmyer-Meshkov instability RMI [1960, 1969] occurs when a shock wave impulsively accelerates a perturbed interface between two gases of different densities. The interaction of the shock wave with the perturbated interface induces the production of vorticity through baroclinic effects, which can give rise to turbulent mixing. The RMI is important in inertial confinement fusion (ICF) experiments and also finds applications in natural phenomena like supernova explosion and supersonic combustion (M. Brouillette [2002]). Several experimental investigations on turbulent mixing zones (TMZ) in shock tubes of different geometrical configurations have been previously carried out. The experiments of M. Vetter and B. Sturtevant [1995] were conducted in a large horizontal shock tube 27x27cm^2 using air and sulphurhexafluoride (SF6) in order to reduce the wall boundary layer effects. L. Erez et al [2000] studied the effect of the membrane which initially separates the two fluids in a fully mixing zone in a smaller horizontal shock tube (8x8cm^2). Various configurations were investigated in order to test the dependence of the thickness of the membrane on the growth rate of the TMZ, and a very good agreement was observed between this work and the results published by M. Vetter and B. Sturtevant [1995]. Similar studies have also been carried out by L. Houas and I. Chemouni [1996], E. Leinov et al. [2009] and K.O Mikaelian [1989, 2011].

In the present work, two-components Laser Doppler Velocimetry (LDV) and Time-resolved Schlieren visualizations are used in order to characterize the turbulent mixing zone induced by RMI and to describe and quantify the development and the growth rate of the interfacial hydrodynamic instability.

EXPERIMENTAL SET-UP

The experimental apparatus used in this study consits of a shock tube operated at the Institut Supérieur de l'Aéronautique et de l'Espace (ISAE). A schematic of the tube is given in figure 1. The shock tube is vertical, 5 m long, and has an internal square cross section of 130 x 130 mm^2. It is composed of three main sections: the high (driver) and low (driven) pressure chambers filled with air, and the test section, which is a second low pressure module filled with SF6 (cf. figure 1). The length of the test section has been fixed to L=250 mm. Transparent windows were installed in the test section of the shock tube in order to enable flow visualization. The incident Mach 1.2 shock wave is generated by impacting a Mylar diaphragm, initially separating the driver and the driven sections of the shock tube, using a blade cutting device. The shock tube length is sufficient to stabilize the shock wave prior to travelling the test section. For studies involving RMI and the resulting turbulent mixing, a thin nitrocellulose membrane (0.5mm thick), which forms the initial interface between air and sulphurhexafluoride (SF6), is trapped between two grids, the upper one imposing a three-dimensional sinusoidal initial perturbation of wavelength equal to 1.8mm. The Atwood number is initially fixed to $A = (\rho SF6 - \rho air) / (\rho SF6 + \rho air) = 0.699$. It is assumed that a perturbation with this wavelength induces a fully developed turbulence in a short time compared to the travelling time of the shock in the test section (J.-F. Haas et al. [2009], private communication). The nitrocellulosic membrane is torn when the incident shock wave interacts with the grids and it should be pointed out that it does not perturb the geometry and the motion of the transmitted shock wave into the SF6.

Vertical mean and fluctuating velocities, denoted U and u' respectively, are measured inside the shock tube using Laser Doppler Velocimetry (LDV). The measurement setup is a Dantec Flow Dynamics commercial system consisting of a continuous 400 mW Argon laser, a Bragg cell, an emitting head with a 300 mm focal length lens and a collecting head with a 300 mm focal length lens. The Bragg cell, set at 40 MHz, is used to shift the Doppler frequency, and enables to measure positive and negative velocity components. The two measurement volumes, of approximate dimensions DX = 47µm, DY = 47µm, DZ = 875µm, are located at the center of the test section of the tube, 43mm above the position of the initial air/SF6 interface. The fluid is seeded with spherical olive oil particles. Their mean Sauter diameter (D32) is 1µm (D32). Pressure histories of the flow in the shock tube are obtained using five flush-mounted piezoelectric pressure transducers. The acquisition frequency was fixed to 2.5MHz. For each shot, the incident Mach number is determined via the two pressure transducers PPT1 and PPT2 located 315 and 115 mm below the interface respectively. In the test section, three additional pressure transducers PPT3, PPT4 and PPT5 are located at 43, 213 and 250mm above the interface respectively. The PPT3 pressure and LDV measurements were triggered on the PPT1 pressure signal. This allows to achieve phase-averaged statistics based on the crossing instant of the incident shock in the measurement volume. Time-resolved Schlieren visualizations are simultaneously operated. Videos of the travelling shock wave and the resulting series of compression/expansion waves inside the test section are recorded thanks to a Phantom V12 high-speed camera. The data rate of the images recording is fixed to 27000 images per second.

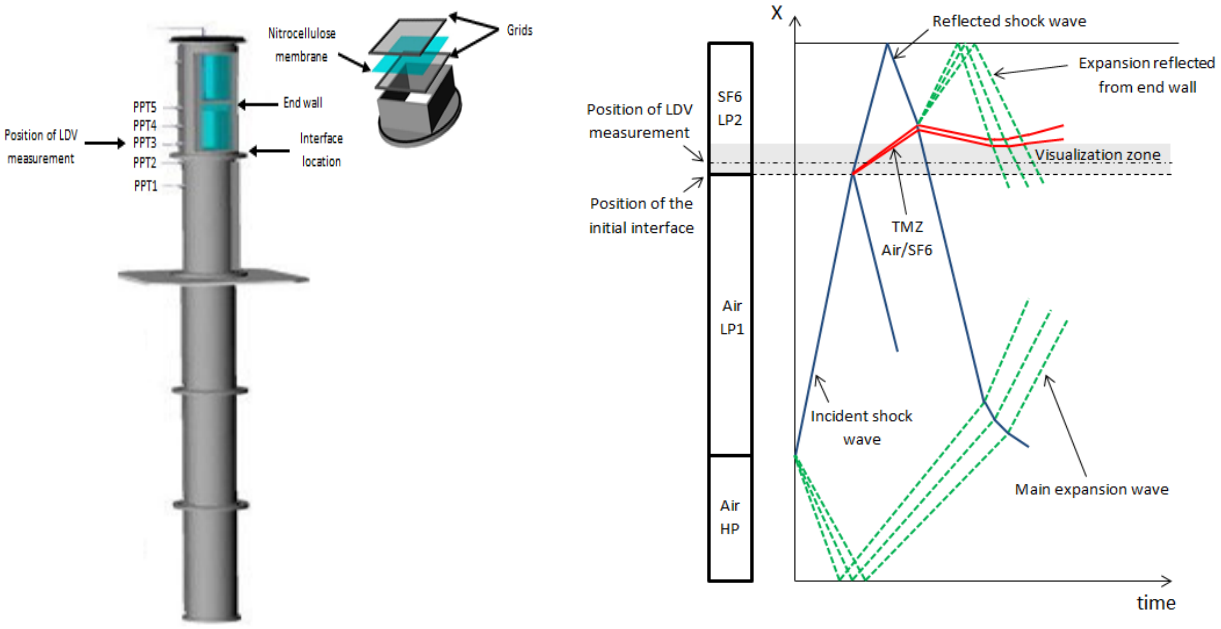

(a) (b)

Figure 1. Sketch of the experimental apparatus (a) and (x-t) diagram of an air/SF6 shot (b)

RESULTS

We describe in this section the experimental results obtained from both the LDV measurements and Time-resolved Schlieren visualizations. Figure 2 depicts the time evolution of the instantaneous vertical velocity measured at x=43 mm, for the air/SF6 configuration. The velocity measurement location allows us to observe the TMZ in the early stage of its development. The Mach number M of the incident shock wave is set to M= 1.203 in air. The resulting Mach number of the SF6-transmitted shock wave is equal to 1.3, thus accelerating the flow to about 73.52 m/s. The mixing zone passes through the measurement location 585µs after the passage of the transmitted shock wave at the LDV measurement volume. At that time, the thickness of the TMZ can be estimated to h=7mm, based on Schlieren images. Therefore, the crossing of the TMZ through the measurement volume lasts 95µs. From Figure 2, it can be seen that the duration of the blackout (Doppler signals cuts) lasts 325 µs. We can thus conclude that membrane fragments still cross the LDV measurement volume after the passage of the TMZ, cutting the Doppler signals for an additional time duration of 230 µs. In the region of interest, located between the incident and the reflected shock waves, data acquisition rates above 180 kHz in pure SF6 were obtained for the U velocity before the blackout and 320 kHz in pure air after the blackout. However, we found that the membrane fragments dramatically reduce the data rate acquisition in the mixing zone. According to our data rate acquisition in the mixing zone, many identical runs are thus needed to get statistically converged measurements. This requires to ensure both repeatability and reproductibility of the experiments, in particular in terms of incident Mach number (M=1.2 ± 1%) and purity of gases.

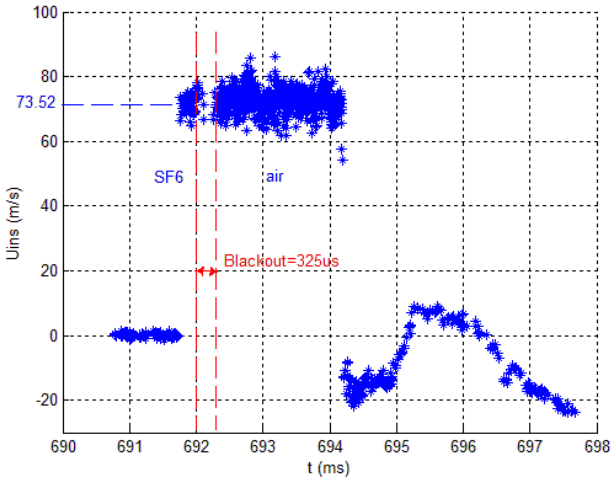

Figure 2. Time evolution of the instantaneous vertical velocity (along the X axis) of an air/SF6 shot at the position x=43mm

For the characterization of the air/SF6 mixing, 35 shots were conducted and the mean and fluctuating, phase-averaged, U and u' velocities were computed. Time discretization into consecutive time windows was fixed to 10µs around the incident and reflected shocks and to 40µs elsewhere. Those time steps were determined as a compromise between sufficiently high number of samples per time step (imposing a minimum temporal width), and the time-filtering effect induced by too large time steps. Convergence of the first and second order statistics was demonstrated to be obtained for samples numbers above 100 in each time window (Figure 3). Figure 4 reveals that this was achieved in most of the region of interest located between the incident and reflected shocks except inside the blackout where large membrane fragments temporarily cross the LDV measurement volume and cut the Doppler signals. Figure 4 depicts the evolution of the phase-averaged mean and fluctuating vertical velocities. The gases are first accelerated at 74m/s after the interaction of the incident shock wave with the initial interface (t_1=0.92ms) then slow down to -18 m/s after TMZ/reflected shock wave interaction (occuring at t_2=3.4ms). They are accelerated once again at 5m/s after the arrival of the expansion reflected from the end wall at t_3=4.64ms (cf. Figure 4.a). The plateau between the incident and reflected shock waves is characterised by three zones: A, B and C (Figure 4.b). In zone A (pure SF6), before the passage of the TMZ, the root-mean square (rms) vertical fluctuating velocity equals u'=3.6m/s. This value is close to the one obtained in air/air experiments (u'=3.4m/s, see G. Bouzgarrou et al. [2011]) and corresponds to the turbulence level of the gas initially located above the grids and below the measurement volume (this fluid volume do not cross the grids). It can be interpreted as the background turbulence level of the experimental set-up. The second zone (denoted zone B) is characterised by the passage of the TMZ, and by the lack of convergence of the statistical approach due to the blackout effect of the membrane fragments. Inside zone C, corresponding to pure air, the value of the rms velocity rises up to 5.33m/s for air/SF6 experiments, whereas it was about 8m/s for pure air configurations. However, in terms of turbulence rate (u'/U), we found that the turbulence intensity is equal to 7.5% for both sets of experiments (air/air and air/SF6 experiments). Indeed, in the case of air/air experiments, the transmitted shock wave is equal to 412 m/s, thus accelerating the flow to about U=107m/s (see G. Bouzgarrou et al. [2011]). However, in the case of air/SF6 experiments, the transmitted shock wave is equal to 176 m/s, thus accelerating the flow to about U=74m/s.

A summary of the vertical fluctuating velocities for air/air and air/SF6 experiments are presented in table 1.

Table 1
Vertical fluctuating velocities for air/air and air/SF6 experiments

	air/air experiments (m/s)	Air/SF6 experiments (m/s)
Zone A	3.42 (pure air)	3.6 (pure SF6)
Zone B	---	---
Zone C	8 (pure air)	5.33 (pure air)

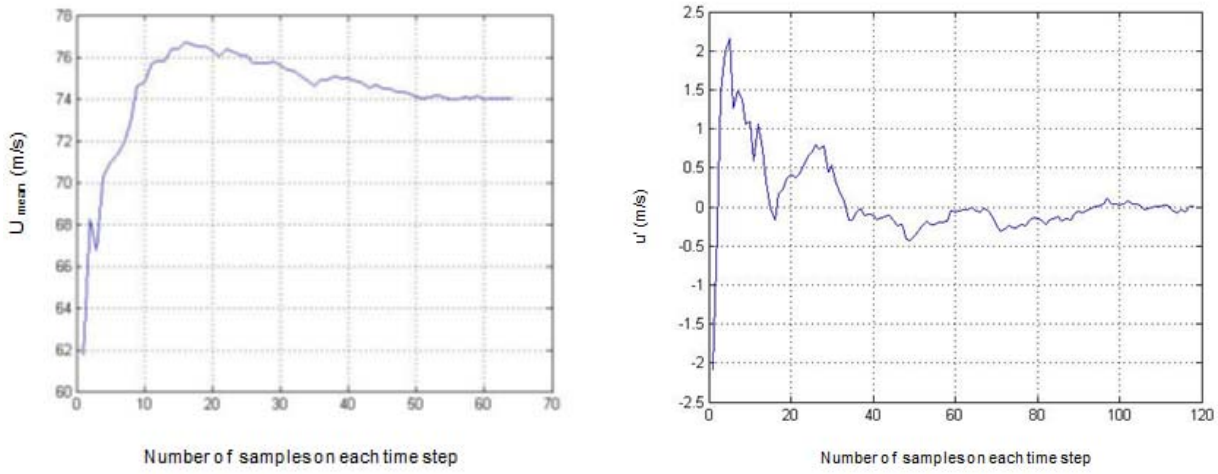

(a) (b)

Figure 3. Convergence of the first order (a) and second order (b) statistics of the vertical velocity

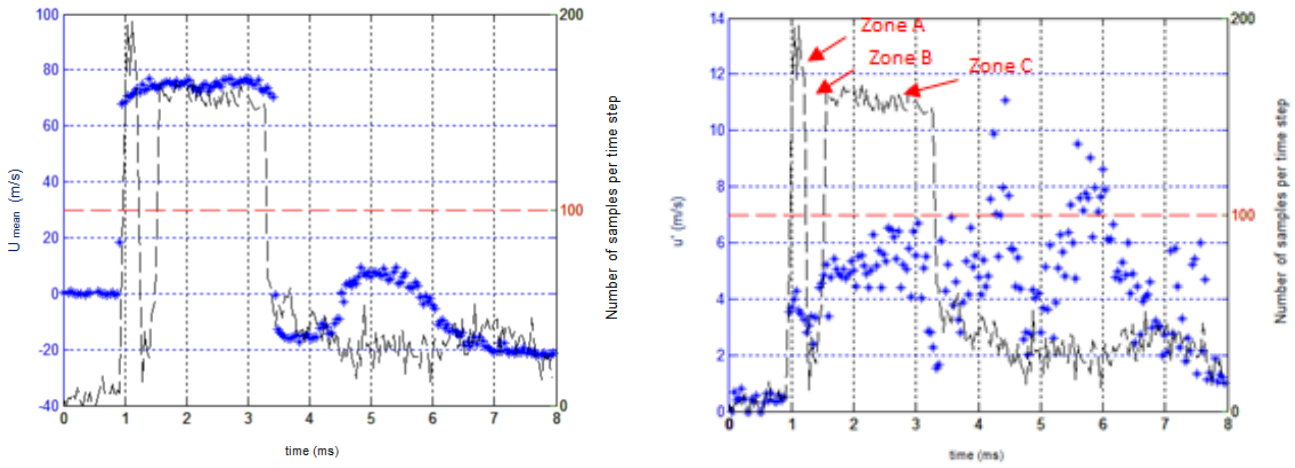

(a) (b)

Figure 4. Evolution of the mean (a) and fluctuating (b) vertical velocity (blue symbols, left vertical axis). Number of samples used for statistics computation, at each time step of the discretized velocity signal (black dashed line, right vertical axis). The red horizontal line corresponds to the number of samples required for statistics convergence.

The evolution of the mean vertical velocity and the corresponding PPT3 pressure signal are illustrated on figure 5. We find chronological consistency between the mean axial velocity and PPT3 pressure signal throughout the whole phenomenon. Before the passage of the transmitted shock wave into SF6 in the measurement volume, the pressure (Pa) and vertical velocity (m/s) are equal to $10^{\wedge 5}$Pa and 0 respectively. Following the passage of the transmitted shock wave in the measurement volume, they rise up to $1.73 \cdot 10^{\wedge 5}$Pa and 74m/s respectively, before reaching $2.47 \cdot 10^{\wedge 5}$Pa and -18m/s after reshock.

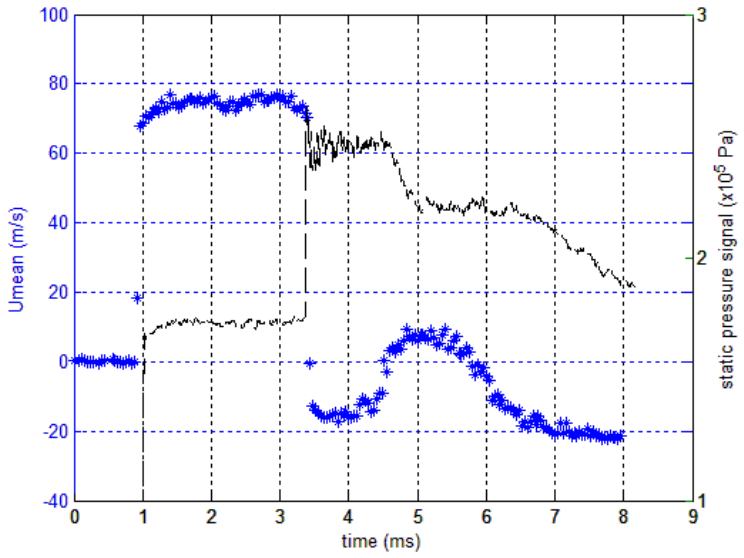

Figure 5. Concurrent evolutions of the mean vertical velocity and PPT3 static pressure

In the present work, the evolution of the mixing zone (MZ) width following the passage of the transmitted shock wave (TSW) into the SF6 is also studied. Figure 6 shows a succession of Schlieren images for an air/SF6 experiment. The time scale in Figure 6 is shifted so that t = 0 is the time when the incident shock wave interacts with the air/SF6 interface. The upward moving transmitted shock wave is clearly seen in figure 6.a. In figures 6.b, c, d, e and f, the TSW continues moving upwards and the MZ grows, separating pure air (on its bottom side) from pure SF6 (on its upper side).

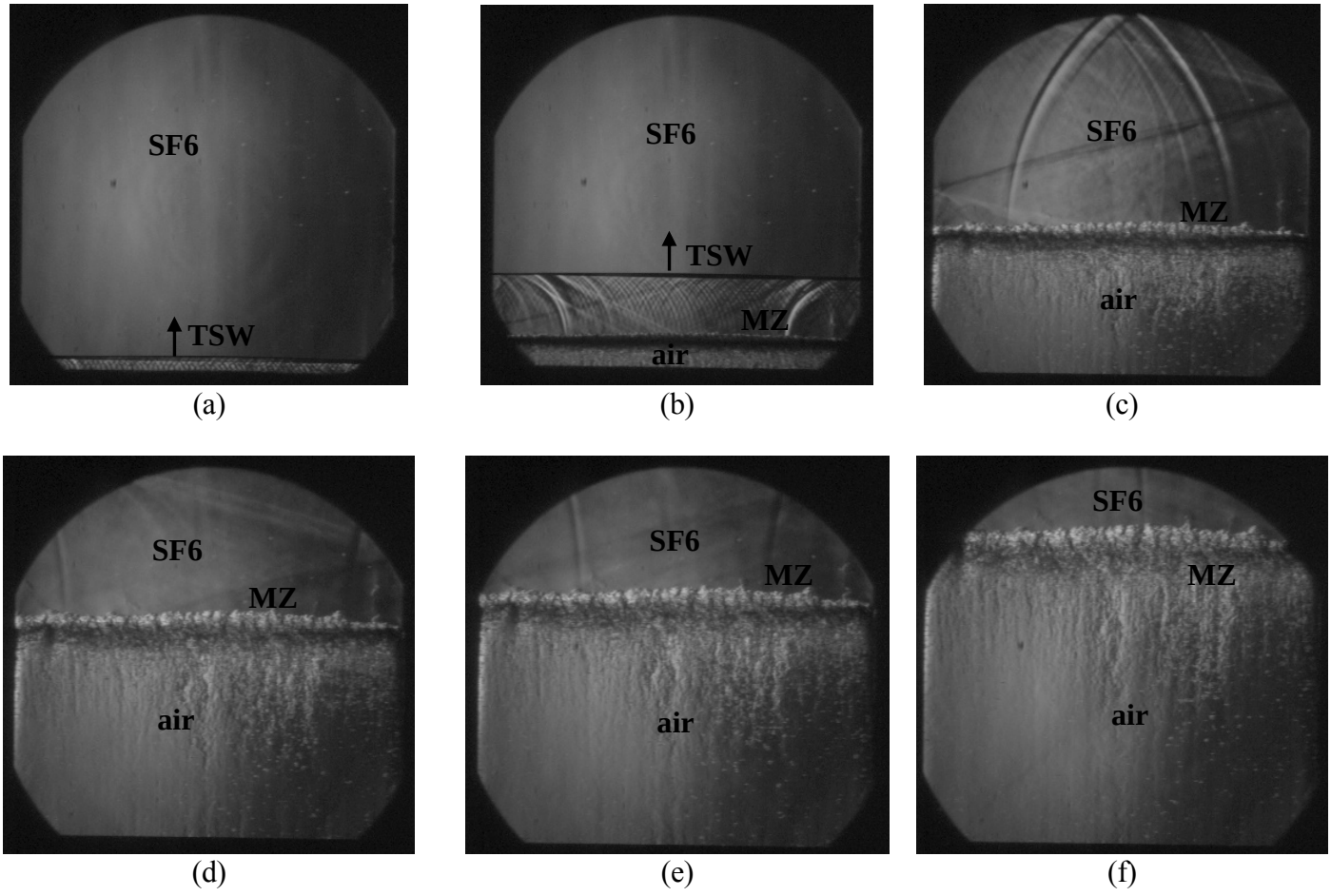

Figure 6. Schlieren images of the MZ generated by the upward moving shock wave: (a) t=0.037ms, (b) t=0.14ms, (c) t=0.7ms, (d) t=0.92ms, (e) t=1.07ms, (f) t=1.33ms.

The thickness of the turbulent mixing zone versus time prior to the arrival of the reflected shock wave is measured from the Schlieren images. A specific image processing algorithm has been developed for this purpose in order to detect mixing boundaries and the time-dependant MZ thickness. In order to reduce noise in each image while preserving edges, a spatial median filter is first used. We then use the Otsu's regional method (figure 7.b) for binarising an image (E. Leinov et al. [2009]). The determination of MZ boundaries is based on the segmentation edge method. More particularly, the Canny filter is used. A region of interest (ROI) is then selected around the MZ inside each image, generally near the center of the tube in order to eliminate wall effects. For each Column of the ROI, two pixels can be found as the boundaries, one on each side of the MZ. Therefore, the width of MZ in each column is obtained by subtracting the longitudinal coordinate of these two pixels. The overall width of the MZ is finally obtained by averaging all the widths of the MZ in all columns of the ROI.

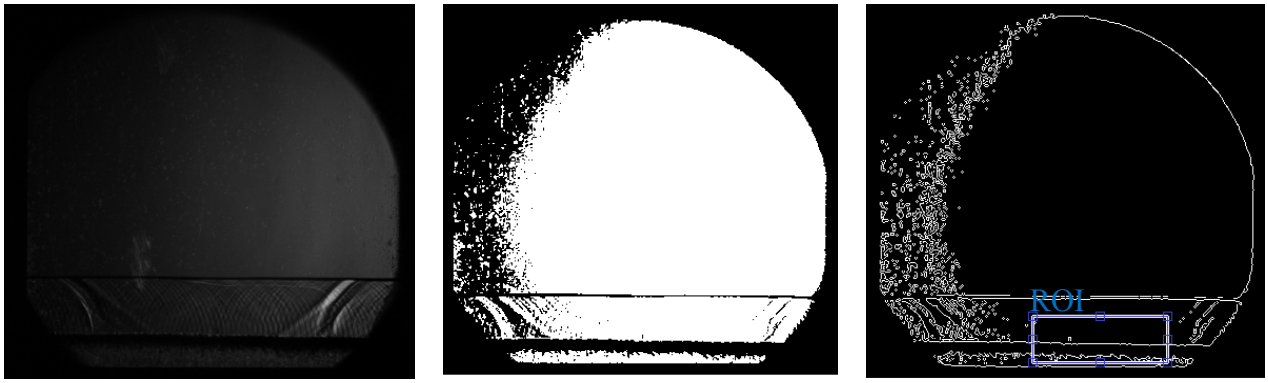

(a) (b) (c)

Figure 7. Turbulent mixing zone thickness determination: (a) Schlieren image, (b) Output of Otsu's method, (c) Output of the Canny filter and choice of the ROI

Figure 8 depicts the evolution of the mixing zone thickness h(t) following the passage of the incident shock wave through the initial air/SF6 interface. It is found that the mixing zone grows asymptotically with time, following a law of the form: $h(t) \approx 9.737\ t^{0.645}$. In addition, the initial growth rate of the MZ calculated by applying a linear interpolation between t=0, corresponding to the initial interface, and t=0.1ms, where the MZ is found to be 2mm thick, is equal to 20m/s. K.O. Mikaelian [1989] indicates that these growth rate can be estimated as $0.28 \cdot \Delta U \cdot A'$; where the empirical growth coefficient 0.28 is based on the MZ growth rate obtained from Rayleigh-Taylor instability experiments, ΔU is the jump in velocity across the interface induced by the incident shock wave and A' is the post-shock Atwood number. In the present study, ΔU is equal to 74m/s and A'= 0.7. Therefore the growth rate, following Mikaelian's model, is found to be 14.5m/s. The discrepancy between the growth rate obtained with Mikaelian's model and the growth rate calculated from our experimental results can be attributed to the calibration of Mikaelian's coefficient (0.28) that has been obtained empirically with Rayleigh-Taylor experiments, and may not be well suited in the present RMI configuration. Following E. Leinov et al. [2009], the growth coefficient is in the range of 0.28-0.39. Here, it equal to 0.38.

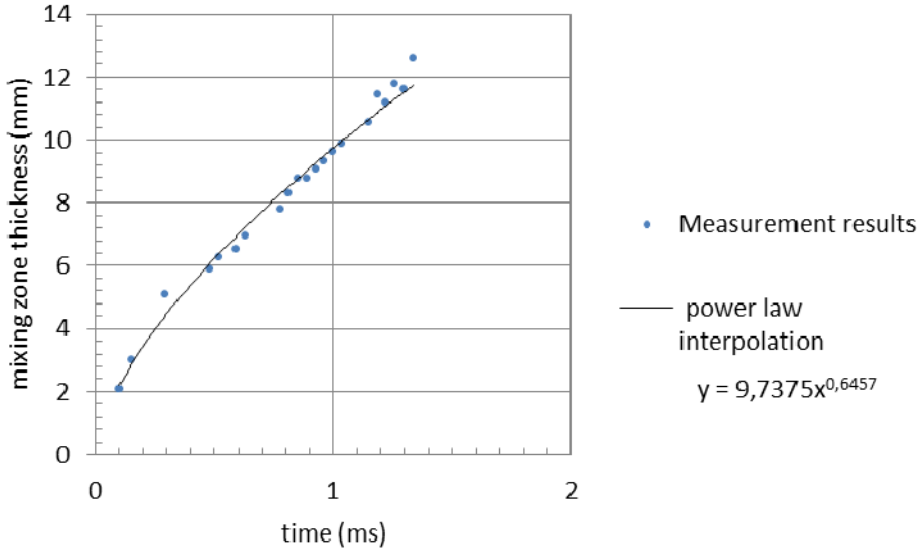

Figure 8. Measurements of the mixing zone thickness

CONCLUSION

In the present work, the air/SF6 turbulent mixing induced by the Richtmyer-Meshkov instability has been studied by means of Laser Doppler Velocimetry (LDV) measurements and Time-resolved Schlieren visualizations. More particularly, 35 shots were conducted and the mean U and fluctuating u' velocity were computed at the position x=43mm above the initial air/SF6 interface. Convergence of the first and second order statistics was achieved in most of the region of interest located between the incident and reflected shocks except inside the blackout where large membrane fragments temporarily cross the LDV measurement volume and cut the Doppler signals. A comparison of turbulence levels between air/air and air/SF6 configurations has been carried out. In order to quantify the growth rate of the turbulent mixing zone induced by RMI, Time-resolved Schlieren visualizations have been operated. A specific image processing algorithm has been developed for this purpose in order to detect mixing boundaries and the time-dependant MZ thickness. It is based on the spatial segmentation edge method. A power law growth of the MZ thickness was found. In the future, we propose to extract the thickness of the turbulent mixing zone using a frequency filter instead of the spatial Canny filter in order to provide a spectral analysis of the Schlieren image content. It can be a very useful analysis tool, both for describing the contents of an image and as an aid in the construction of imaging filters. In addition, we propose to study the air/SF6 mixing consecutive to the passage of the reflected shock wave.

ACKNOWLEDGMENTS

This work is supported by CEA, DAM, DIF under grant number 09-37-C-SACO.

REFERENCES

Bouzgarrou, G., Bury, Y., Jamme, S., Haas, J.F., Counilh, D., Cazalbou, J.B., [2011]. Experimental characterization of turbulence produced in a shock tube: a preliminary work for the study of the turbulent gaseous mixing induced by the Richtmyer-Meshkov Instability, *ISSW28*, 17-22 July 2011 Manchester.

Brouillette, M. [2002]. The Richtmyer-Meshkov instability. *Annu. Rev. Fluid Mech*, Vol. 34, pp 445-468.

Erez, L., Sadot, O., Oron, D., Erez, G., Levin, L.A., Shvarts, D., Ben Dor, G. [2000]. Study of the membrane effect on turbulent mixing measurements in shock tubes. *Shock waves*, Vol. 10, pp 241-251.

Houas, L., Chemouni, I. [1996]. Experimental investigation of Richtmyer-Meshkov instability in shock tube. *Phys. Fluids* 8 (2), pp 614-627.

Haas, J.-F., Counilh, D., Poggi, F., Rodriguez, G., Houas, L., Jourdan, G., Mariani, C., Schwaerdelé, L. [Août 2009]. Mesures de mélanges turbulents en tube à chocs. *Chocs - Revue scientifique et technique de la direction des applications militaires*, Numéro 37.

Leinov, E., Malamud, G., Elbaz, Y., Levin, L.A., Ben Dor, G., Shvarts, D., Sadot, O. [2009]. Experimental and numerical investigation of the Richtmyer-Meshkov instability under reshock conditions. *J. Fluid Mech.*, Vol. 626, pp 449-475.

Meshkov, E.E. [1969]. Instability of the interface of two gases accelerated by a shock wave. *Sov. Fluid Dyn.*, Vol. 4, pp 101-108.

Mikaelian, K.O. [2011]. Extended model for Richtmyer-Meshkov mix. *Physica D*, Vol. 240, pp 935-942.

Mikaelian, K.O. [1989]. Turbulent mixing generated by Rayliegh-Taylor and Richtmyer-Meshkov instabilities. *Physica D*, Vol. 36, pp 343-357.

Richtmyer, R.D. [1960]. Taylor instability in shock acceleration of compressible fluids. *Comm. Pure Appl. Math.*, Vol. 8, pp 297-319.

Vetter, M.,Sturtevant, B. [1995]. Experiments on the Richtmyer-Meshkov instability of an air/SF6 interface. *Shock waves*, Vol. 4, pp 247-252.